JAERI-M
89-107

NEANDC(J)-139/U
INDC(JPN)-126/L

MEASUREMENTS OF DIFFERENTIAL CROSS SECTIONS FOR THE REACTIONS ^{6,7}LI(N, D)^{5,6}HE AND ^{6,7}LI(N, T)^{4,5}HE AT 14.1 MEV

August 1989

Shoji SHIRATO*, Shinji SHIBUYA**, Kazuhiro HATA*
Yoshiaki ANDO* and Keiichi SHIBATA

日本原子力研究所
Japan Atomic Energy Research Institute

JAERI-Mレポートは，日本原子力研究所が不定期に公刊している研究報告書です。
入手の問合わせは，日本原子力研究所技術情報部情報資料課（〒319-11茨城県那珂郡東海村）あて，お申しこしください。なお，このほかに財団法人原子力弘済会資料センター（〒319-11茨城県那珂郡東海村日本原子力研究所内）で複写による実費頒布をおこなっております。

JAERI-M reports are issued irregularly.
Inquiries about availability of the reports should be addressed to Information Division Department of Technical Information, Japan Atomic Energy Research Institute, Tokai-mura, Naka-gun, Ibaraki-ken 319-11, Japan.

編集兼発行　日本原子力研究所
印　　刷　いばらき印刷㈱

JAERI-M 89-107

Measurements of Differential Cross Sections for the Reactions $^{6,7}Li(n,d)^{5,6}He$ and $^{6,7}Li(n,t)^{4,5}He$ at 14.1 MeV

Shoji SHIRATO*, Shinji SHIBUYA**, Kazuhiro HATA*
Yoshiaki ANDO* and Keiichi SHIBATA

Department of Physics
Tokai Research Establishment
Japan Atomic Energy Research Institute
Tokai-mura, Naka-gun, Ibaraki-ken

(Received July 21, 1989)

A summary of our measured cross sections for the 14.1 MeV neutron-induced reactions on lithium isotopes has been presented. Our data were measured with two counter telescopes, each of which consisted of two gas proportional counters and silicon ΔE and E detectors. Measured energy spectra of deuterons and tritons from $^{6}Li(n,d)n^{4}He$ and $^{7}Li(n,t)n^{4}He$, respectively, were analyzed by a simple final-state interaction theory. Measured angular distributions for these reactions as well as $^{6}Li(n,t)^{4}He$ and $^{7}Li(n,d)^{6}He$ were analyzed by exact finite-range distorted wave Born approximation (EFR-DWBA) calculations. Spectroscopic factors extracted from the EFR-DWBA analyses have been compared with theoretical predictions.

Keywords: Neutron Nuclear Data, E_n = 14.1 MeV; ^{6}Li and ^{7}Li, Enriched Target; Measured $\sigma(\theta,E)$ and $\sigma(\theta)$; DWBA, Spectroscopic Factor

---

This report is written by summarizing the effort implemented under the Research-in-Trust in 1987 - 1988 fiscal years from the Japan Atomic Energy Research Institute (JAERI).

* Rikkyo University

** Sumitomo Heavy Industries, Ltd.

14.1 MeVでの反応^{6,7}Li(n,d)^{5,6}Heと^{6,7}Li(n,t)^{4,5}Heの微分断面積の測定

日本原子力研究所東海研究所物理部
白土　鈔二*・渋谷　真二**・秦　和博*・安藤　嘉章*・柴田　恵一

（1989年7月21日受理）

リチウム同位体に関する14.1 MeV中性子誘起核反応断面積の測定結果についてまとめた。われわれのデータは二つのカウンターテレスコープを用いて得られた。このテレスコープは2個のガス比例計数管とシリコンΔEとE検出器からなっている。^{6}Li(n,d)n^{4}Heと^{7}Li(n,t)n^{4}Heからのそれぞれ重陽子と三重陽子の測定されたエネルギースペクトルは簡単な終状態相互作用理論によって解析された。これらの反応および^{6}Li(n,t)^{4}Heと^{7}Li(n,d)^{6}Heの測定された角分布は，正確な有限レンジひずみ波Born近似（EFR－DWBA）計算によって解析された。EFR－DWBA解析から導かれた分光学的因子は理論計算と比較されている。

この報告書は日本原子力研究所からの昭和62－63年度委託研究で行なわれた成果をまとめたものである。
東海研究所：〒319－11　茨城県那珂郡東海村白方字白根2－4
* 立教大学
** 住友重機械工業株式会社

Contents

目　　次

1. Introduction

Experimental data on the fast-neutron induced reactions for the emission of charged particles from lithium isotopes ^{6,7}Li are very important to investigate not only the reaction mechanism and the cluster structure in nuclear physics but also the fusion reactor in nuclear engineering. However, the data and analyses of absolute cross sections for these reactions are very scarce even at the present time.

Previously, we measured the differential cross sections for the reactions ^{6}Li(n,d)^{5}He and ^{6}Li(n,t)^{4}He at 14.1 MeV in a limited angular region and compared our data with the calculations of exact finite-range distorted wave Born approximation (EFR-DWBA)[1]. Since then, we have continued to obtain the absolute cross section data not only on ^{6}Li[2,3] in a wider angular region but also on ^{7}Li[4,5,6]. As mentioned in a previous paper[5], some discrepancies between experimental data and EFR-DWBA calculations were found at some angles. A remeasurement[6] was required to obtain more accurate energy spectra of tritons and deuterons especially from ^{7}Li bombarded by 14.1 MeV neutrons. As the result of these efforts, it was found that our data were in fairly well agreement with the data of Zagreb group[7-10] using 14.4 MeV neutrons in some angular ranges and generally could be reproduced to some extent over measured angular ranges by EFR-DWBA calculations, yielding information about spectroscopic factors on the basis of the particle pickup mechanism.

In this paper, we present a summary of our experimental data[1-6] on the one- or two-nucleon transfer reactions for ^{6,7}Li, comparing with the Zagreb data of 14.4 MeV in some figures as well as with the EFR-DWBA predictions to derive spectroscopic factors. In sect. 2, we also

describe the details of our newly performed experiment[6], in which we aimed to settle the $^{7}Li(n,d)^{6}He$ data of relatively small cross sections (less than 1 mb/sr).

2. Experimental procedures

The procedures of our series experiments using 95.58% enriched ^{6}Li metal targets of various thicknesses ranged from 2.35 to 3.74 mg/cm^2 and a preliminary one using a 12.44 mg/cm^2 natural lithium metal target have been reported in a previously published paper[1] and unpublished ones[2,3,4]. These experiments have been performed using an old 200 kV Cockcroft-Walton accelerator of Rikkyo University. As mentioned in sect. 1, here we describe only our most recent experiment on ^{7}Li using a newly constructed 300 kV Cockcroft-Walton accelerator[11] for the production of the ^{3}H-d neutrons of 14.1 MeV.

The absolute determination of neutron yields in this experiment was performed with an accuracy of about 2% by use of the associated α-particle method using a Si p-i-n photodiode (Hamamatsu S1723-06) as the α-monitor and a ^{3}H-Ti-Cu target (Amersham TRT-31, 2.4 Ci). The details of this method have been described elsewhere[11]. Another Si p-i-n photodiode (Hamamatsu S1722) and a NE213 liquid scintillator, which were placed at 3 cm and 100 cm respectively from the neutron source point, were employed as neutron monitors. An accelerated deuteron beam of 170 keV was collimated by passing through two collimators of 3 mm and 2 mm in diameter after focusing by Q-magnets.

A 3.90 ± 0.06 mg/cm^2 target of 99.988% enriched ^{7}Li metal was prepared by rolling[6] and placed on the upper hole of a target holder (Al or Ta) with two holes of 5.9 mm in diameter. This target was placed

describe the details of our newly performed experiment[6], in which we aimed to settle the $^{7}Li(n,d)^{6}He$ data of relatively small cross sections (less than 1 mb/sr).

2. Experimental procedures

The procedures of our series experiments using 95.58% enriched ^{6}Li metal targets of various thicknesses ranged from 2.35 to 3.74 mg/cm^2 and a preliminary one using a 12.44 mg/cm^2 natural lithium metal target have been reported in a previously published paper[1] and unpublished ones[2,3,4]. These experiments have been performed using an old 200 kV Cockcroft-Walton accelerator of Rikkyo University. As mentioned in sect. 1, here we describe only our most recent experiment on ^{7}Li using a newly constructed 300 kV Cockcroft-Walton accelerator[11] for the production of the ^{3}H-d neutrons of 14.1 MeV.

The absolute determination of neutron yields in this experiment was performed with an accuracy of about 2% by use of the associated α-particle method using a Si p-i-n photodiode (Hamamatsu S1723-06) as the α-monitor and a ^{3}H-Ti-Cu target (Amersham TRT-31, 2.4 Ci). The details of this method have been described elsewhere[11]. Another Si p-i-n photodiode (Hamamatsu S1722) and a NE213 liquid scintillator, which were placed at 3 cm and 100 cm respectively from the neutron source point, were employed as neutron monitors. An accelerated deuteron beam of 170 keV was collimated by passing through two collimators of 3 mm and 2 mm in diameter after focusing by Q-magnets.

A 3.90 ± 0.06 mg/cm^2 target of 99.988% enriched ^{7}Li metal was prepared by rolling[6] and placed on the upper hole of a target holder (Al or Ta) with two holes of 5.9 mm in diameter. This target was placed

3.0 cm from the neutron source point at the center of a scattering chamber[12]. In the chamber, two counter telescopes (CT1 and CT2) were placed 4.6 cm from the lithium target. A collimator of 5 mm in diameter was located in front of the ΔE detector of each counter telescope for defining the solid angle, as seen in fig. 1. Each counter telescope consisted of two gas proportional counters and silicon ΔE and E detectors. The counter gas of Ar with 5% of CO_2 was filled to a pressure of 100 Torr in the chamber. The experimental arrangement as well as the thicknesses of the silicon ΔE and E detectors is shown schematically in fig. 1.

A block diagram of the electronic system used in this experiment is shown in fig. 2. Energy and time signals from eight detectors, viz. two counters (PC_{11}, PC_{12}) and 32 μm and 1500 μm Si detectors ($Si\Delta E_1$, SiE_1) for CT1, and two counters (PC_{21}, PC_{22}) and 16 μm and 1500 μm Si detectors ($Si\Delta E_2$, SiE_2) for CT2, were taken as list mode data on magnetic tape by a CAMAC data acquisition system, after being treated by a NIM-module electronic system. The multiparameter event data were analyzed in real-time for particle identification, and the energy spectra of separated charged particles (p, d, t and ^{4}He) were obtained in the off-line analysis. The particle identification was almost completely performed, as seen in fig. 3-a (with target) and -b (without target) for the telescope setting angle $\theta_0 = 0^\circ$ and also in fig. 3-c (with target) and -d (without target) for $\theta_0 = 50^\circ$, which illustrated the typical examples of a plot of energy E vs energy loss ΔE.

In our series experiments, the absolute cross sections for ^{6}Li have been determined with overall accuracies of about ±5 - 11% for the (n,d) case and ±7 - 14% for the (n,t) case in the measured angular range from 0° to 130°. These uncertainties include the systematic error originated

from the uncertainties in target thickness (±1 - 3%), geometry (±3%) and neutron flux (±2%). The absolute cross sections for ^{7}Li were determined with the statistical errors of about ±4 - 32% for (n,t) and of about ±40% for (n,d) in the measured angular range from 0° to 80°. These data on ^{7}Li do not include the systematic error mentioned above.

3. Results and discussion

The energy spectra of deuterons and tritons from the reactions ^{6}Li(n,d)^{5}He and ^{7}Li(n,t)^{5}He, respectively, were measured at various telescope setting angles in the ranges from 0° to 130° for ^{6}Li and to 80° for ^{7}Li. These experimental data for the final three-particle reactions are tabulated in the appendix (tables A1 and A2). Typical examples of the measured energy spectra are shown in fig. 4. The energy spectrum observed at a forward angle shows a remarkable peak due to the final state interaction (FSI) especially at the high energy end, as seen in fig. 4. The curves drawn in fig. 4 are the results of calculations taking into account n-α, n-t and t-α FSIs, which are represented by the phase-shifts $\delta^{2J}{}_{L}$ of L-wave scattering in the unobserved pair subsystem of total angular momentum J in the final state. An energy resolution of 800 keV has been folded into the curves of fig. 4. Both the deuteron- and the triton-energy spectra are dominated by the FSI effects of the well-known $P_{3/2}$ n-α scattering at the high energy end. In this energy region, the Lehman effect of the n-α plane-wave final-state component[13] does not appear to be significant. In the case of the triton energy spectrum, the significant enhancement due to the t-α FSI appears in the middle energy region, as seen in fig. 4. The corresponding d-α FSI enhancement in the case of the deuteron energy spectrum for ^{6}Li should

from the uncertainties in target thickness (±1 - 3%), geometry (±3%) and neutron flux (±2%). The absolute cross sections for ^{7}Li were determined with the statistical errors of about ±4 - 32% for (n,t) and of about ±40% for (n,d) in the measured angular range from 0° to 80°. These data on ^{7}Li do not include the systematic error mentioned above.

3. Results and discussion

The energy spectra of deuterons and tritons from the reactions ^{6}Li(n,d)^{5}He and ^{7}Li(n,t)^{5}He, respectively, were measured at various telescope setting angles in the ranges from 0° to 130° for ^{6}Li and to 80° for ^{7}Li. These experimental data for the final three-particle reactions are tabulated in the appendix (tables A1 and A2). Typical examples of the measured energy spectra are shown in fig. 4. The energy spectrum observed at a forward angle shows a remarkable peak due to the final state interaction (FSI) especially at the high energy end, as seen in fig. 4. The curves drawn in fig. 4 are the results of calculations taking into account n-α, n-t and t-α FSIs, which are represented by the phase-shifts $\delta^{2J}{}_{L}$ of L-wave scattering in the unobserved pair subsystem of total angular momentum J in the final state. An energy resolution of 800 keV has been folded into the curves of fig. 4. Both the deuteron- and the triton-energy spectra are dominated by the FSI effects of the well-known $P_{3/2}$ n-α scattering at the high energy end. In this energy region, the Lehman effect of the n-α plane-wave final-state component[13] does not appear to be significant. In the case of the triton energy spectrum, the significant enhancement due to the t-α FSI appears in the middle energy region, as seen in fig. 4. The corresponding d-α FSI enhancement in the case of the deuteron energy spectrum for ^{6}Li should

exist in an unobserved low-energy region. Thus, in the case of the reaction consisting of three particles in the final state, the measured energy spectrum must be analyzed for each FSI channel in a three-body model and also corrected for any unobserved low-energy part, before the energy integration of the double differential cross section obtained is carried out, in order to compare the experimental result with DWBA calculations.

The measured and analyzed data on the differential cross section for the $^{6}Li(n,d)^{5}He(P_{3/2})$ reaction in the center-of-mass (c.m.) system are summarized in fig. 5 and also table 1. The cross section data[1] at each angle has been obtained from the measured energy spectrum by making a correction for the unobserved lower-energy region on the basis of the Watson-Migdal form. The curve drawn in fig. 5 is the result of the EFR-DWBA calculation[1]. The sharp rise in the backward angular distribution predicted by the EFR-DWBA calculation is in favor of our data[3].

The measured data on the c.m. differential cross section for the $^{6}Li(n,t)^{4}He$ reaction are summarized in fig. 6 and also table 1. The curves in fig. 6 are the result of the EFR-DWBA calculations in both cases of the incoherent sum of the d-pickup amplitudes only (the solid line)[1] and the coherent sum between the d-pickup and ^{3}He-pickup amplitudes (the dashed line)[2].

The optical potential parameters used in the EFR-DWBA calculations are summarized[5] in table 2 for the n-^{6}Li and the n-^{7}Li reactions in our works. We used the optical potentials of Hyakutake et al.[14] for the entrance channels of n-^{6}Li and n-^{7}Li. All the EFR-DWBA calculations in our works have been performed by using the code DWUCK[15].

The data on the c.m. differential cross sections for the reactions

$^{7}Li(n,d)^{6}He(g.s., 0^{+})$ and $^{7}Li(n,d)^{6}He^{*}(1.80\ MeV, 2^{+})$ are shown in fig. 7 and also table 3. The measured cross section for $^{7}Li(n,d)^{6}He^{*}(1st, 2^{+})$ has been corrected for a contribution from $^{7}Li(n,d)\alpha nn$ by means of the analysis of the measured deuteron energy spectrum[6]. Our previous data[5] on the differential cross section for $^{7}Li(n,d)^{6}He^{*}(1st)$, which are larger in the magnitude by a factor of 3 than the present data[6] as well as than the EFR-DWBA predictions[5], should be revised by the correct reanalysis of background subtraction and/or of the ^{6}He ($\rightarrow \alpha nn$) breakup contribution.

The curves drawn in fig. 7 are the result of EFR-DWBA calculations[5] using the same potential parameters as those of Bingham et al.[16], who obtained the d-^{6}Li potential, for the d-^{6}He exit channels.

The measured data on the c.m. differential cross section for the $^{7}Li(n,t)^{5}He$ reaction are shown in fig. 8 and also table 4. The data[4,6] for $^{7}Li(n,t)^{5}He(P_{3/2})$ have been derived by the same way as that used in the case[1] of $^{6}Li(n,d)^{5}He(P_{3/2})$ without involving a plane-wave final-state component[13] in the n-α scattering state and some FSI channels other than the $P_{3/2}$ n-α channel. The curves in fig. 8 are the result of the EFR-DWBA calculations[5].

Spectroscopic factors were extracted from the experimental data in comparison with the EFR-DWBA results in a similar way to that described in ref. 1. The result of the spectroscopic factors obtained are summarized in table 5 in comparison with shell model predictions[17,18,19] and calculated coefficients of fractional parentage (CFP)[20,21] as well as with three-body cluster model predictions[22]. The present result seems to be almost consistent with the theoretical predictions except the shell model predictions of Cohen and Kurath[17] giving somewhat small factors. A highly accurate analysis would be required to extract more

precise information about spectroscopic factors for ^{7}Li, as performed for the ^{6}Li case[1,23] taking into account state configuration mixing.

4. Conclusions

The differential cross sections for the 14.1 MeV neutron induced reactions of charged-paprticle (d and t) emission from ^{6,7}Li have been measured and summarized in this paper. Our experimental data are in fair agreement with the Zagreb data of 14.4 MeV.

Our experimental data have given clear evidence of the backward increase of the ^{6}Li(n,d)^{5}He cross section, predicting by the EFR-DWBA calculation[1] based on the proton pickup mechanism. Generally, the EFR-DWBA calculations based on the pickup mechanism of one- or two-particle transfer reproduce forward differential cross sections for the (n,d) and (n,t) reactions on ^{6}Li. However, some discrepancies between the experimental data and the DWBA calculations appear over the whole angular region, especially at very backward angles. For example, a coherent sum of the deuteron and ^{3}He pickup amplitudes improves the discrepancy at larger angles than 150° (c.m.) for the ^{6}Li(n,t) case.

The experimental data on ^{7}Li(n,d)^{6}He(g.s.) and ^{7}Li(n,d)^{6}He(1st) are well reproduced by the EFR-DWBA calculations based on the proton pickup mechanism.

A contribution of only the n-α FSI to the cross section data on ^{7}Li (n,t)^{5}He is described dominantly by only the deuteron pickup mechanism. The triton knockon mechanism predicts too small cross sections.

The extracted spectroscopic factors in this work have been compared with the theoretical values, predicting to be almost consistent except the values of Cohen and Kurath. However, because of some discrepancies

precise information about spectroscopic factors for ^{7}Li, as performed for the ^{6}Li case[1,23] taking into account state configuration mixing.

4. Conclusions

The differential cross sections for the 14.1 MeV neutron induced reactions of charged-paprticle (d and t) emission from ^{6,7}Li have been measured and summarized in this paper. Our experimental data are in fair agreement with the Zagreb data of 14.4 MeV.

Our experimental data have given clear evidence of the backward increase of the ^{6}Li(n,d)^{5}He cross section, predicting by the EFR-DWBA calculation[1] based on the proton pickup mechanism. Generally, the EFR-DWBA calculations based on the pickup mechanism of one- or two-particle transfer reproduce forward differential cross sections for the (n,d) and (n,t) reactions on ^{6}Li. However, some discrepancies between the experimental data and the DWBA calculations appear over the whole angular region, especially at very backward angles. For example, a coherent sum of the deuteron and ^{3}He pickup amplitudes improves the discrepancy at larger angles than 150° (c.m.) for the ^{6}Li(n,t) case.

The experimental data on ^{7}Li(n,d)^{6}He(g.s.) and ^{7}Li(n,d)^{6}He(1st) are well reproduced by the EFR-DWBA calculations based on the proton pickup mechanism.

A contribution of only the n-α FSI to the cross section data on ^{7}Li (n,t)^{5}He is described dominantly by only the deuteron pickup mechanism. The triton knockon mechanism predicts too small cross sections.

The extracted spectroscopic factors in this work have been compared with the theoretical values, predicting to be almost consistent except the values of Cohen and Kurath. However, because of some discrepancies

found in detail between theoretical and experimental angular distributions over wide angular regions, further theoretical studies based on DWBA as well as the Faddeev approach should be necessary to extract more precise values of spectroscopic factors especially for ^{7}Li.

Acknowledgments

This work has been financially supported by the 1987 - 1988 Research-in-Trust from the Japan Atomic Energy Research Institute (JAERI), and also in part by the Grant-in-Aid for General Scientific Research (No. 62540214), the Ministry of Education in Japan. The authors are greatly appreciate to Drs. S. Igarasi and T. Asami of the JAERI Nuclear Data Center.

References

1) S. Higuchi, K. Shibata, S. Shirato and H. Yamada, Nucl. Phys. A384, 51 (1982).

2) H. Yamada, Y. Ando and S. Shirato, JAERI Report 1983, NEANDC(J)-94/U, INDC(JAP)-81/U, p.75.

3) Y. Ando, S. Shirato and H. Yamada, JAERI Report 1984, NEANDC(J)-104/U, INDC(JPN)-92/U, p.58.

4) I. Furutate, T. Kokubu, Y. Ando, T. Motobayashi and S. Shirato, JAERI Report 1985, NEANDC(J)-116/U, INDC(JPN)-102/U, p.81; I. Furutate, Master thesis (Rikkyo University, 1986), in Japanese.

5) S. Shirato, S. Shibuya, Y. Ando and K. Shibata, Proc. Int. Conf. on Nuclear Data for Science and Technology (Editor: S. Igarasi, JAERI, 1988) p. 249.

6) S. Shibuya, Master thesis (Rikkyo University, 1989), in Japanese.

found in detail between theoretical and experimental angular distributions over wide angular regions, further theoretical studies based on DWBA as well as the Faddeev approach should be necessary to extract more precise values of spectroscopic factors especially for ^{7}Li.

Acknowledgments

This work has been financially supported by the 1987 - 1988 Research-in-Trust from the Japan Atomic Energy Research Institute (JAERI), and also in part by the Grant-in-Aid for General Scientific Research (No. 62540214), the Ministry of Education in Japan. The authors are greatly appreciate to Drs. S. Igarasi and T. Asami of the JAERI Nuclear Data Center.

References

1) S. Higuchi, K. Shibata, S. Shirato and H. Yamada, Nucl. Phys. A384, 51 (1982).

2) H. Yamada, Y. Ando and S. Shirato, JAERI Report 1983, NEANDC(J)-94/U, INDC(JAP)-81/U, p.75.

3) Y. Ando, S. Shirato and H. Yamada, JAERI Report 1984, NEANDC(J)-104/U, INDC(JPN)-92/U, p.58.

4) I. Furutate, T. Kokubu, Y. Ando, T. Motobayashi and S. Shirato, JAERI Report 1985, NEANDC(J)-116/U, INDC(JPN)-102/U, p.81; I. Furutate, Master thesis (Rikkyo University, 1986), in Japanese.

5) S. Shirato, S. Shibuya, Y. Ando and K. Shibata, Proc. Int. Conf. on Nuclear Data for Science and Technology (Editor: S. Igarasi, JAERI, 1988) p. 249.

6) S. Shibuya, Master thesis (Rikkyo University, 1989), in Japanese.

found in detail between theoretical and experimental angular distributions over wide angular regions, further theoretical studies based on DWBA as well as the Faddeev approach should be necessary to extract more precise values of spectroscopic factors especially for ^{7}Li.

Acknowledgments

This work has been financially supported by the 1987 - 1988 Research-in-Trust from the Japan Atomic Energy Research Institute (JAERI), and also in part by the Grant-in-Aid for General Scientific Research (No. 62540214), the Ministry of Education in Japan. The authors are greatly appreciate to Drs. S. Igarasi and T. Asami of the JAERI Nuclear Data Center.

References

1) S. Higuchi, K. Shibata, S. Shirato and H. Yamada, Nucl. Phys. A384, 51 (1982).

2) H. Yamada, Y. Ando and S. Shirato, JAERI Report 1983, NEANDC(J)-94/U, INDC(JAP)-81/U, p.75.

3) Y. Ando, S. Shirato and H. Yamada, JAERI Report 1984, NEANDC(J)-104/U, INDC(JPN)-92/U, p.58.

4) I. Furutate, T. Kokubu, Y. Ando, T. Motobayashi and S. Shirato, JAERI Report 1985, NEANDC(J)-116/U, INDC(JPN)-102/U, p.81; I. Furutate, Master thesis (Rikkyo University, 1986), in Japanese.

5) S. Shirato, S. Shibuya, Y. Ando and K. Shibata, Proc. Int. Conf. on Nuclear Data for Science and Technology (Editor: S. Igarasi, JAERI, 1988) p. 249.

6) S. Shibuya, Master thesis (Rikkyo University, 1989), in Japanese.

7) V. Valković, G. Paić, I. Slaus, P. Tomas, M. Cerineo and G. R. Satchler, Phys. Rev. 139, B331 (1965).

8) V. Valković, I. Slaus, P. Tomas and M. Cerineo, Nucl. Phys. A98, 305 (1967).

9) D. Rendić and G. Paić, Rossendorf Reports 2, 143 (1967).

10) D. Miljanic, M. Furic and V. Valković, Nucl. Phys. A148, 312 (1970).

11) S. Shirato, S. Shibuya and Y. Ando, RUP-88-1 (Rikkyo University Preprint, unpublished, 1988); S. Shirato, S. Shibuya, Y. Ando, T. Kokubu and K. Hata, Nucl. Instr. and Meth. A278, 477 (1989).

12) S. Shirato, K. Shibata, M. Saito and S. Higuchi, Nucl. Instr. and Meth. 199, 469 (1982).

13) C. T. Christou, D. R. Lehman and W. C. Parke, Phys. Rev. 37, 445, 458 (1988).

14) M. Hyakutake, M. Sonoda, A. Katase, Y. Wakuta, M. Matoba, H. Tawara and I. Fujita, J. Nucl. Sci. Technol. 11, 407 (1974).

15) P. D. Kunz, University of Colorado Report, unpublished.

16) H. G. Bingham, A. R. Zander, K. W. Kemper and N. R. Fletcher, Nucl. Phys. A173, 265 (1971).

17) S. Cohen and D. Kurath, Nucl. Phys. A101, 1 (1967).

18) T. W. Donnelly and J. D. Walecka, Phys. Lett. 44B, 330 (1973).

19) R. D. Lawson, Theory of the nuclear shell model, (Clarendon Press, Oxford, 1980) p. 405.

20) S. Shlomo, Nucl. Phys. A184, 545 (1972).

21) Yu. F. Smirnov and D. Chlebowska, Nucl. Phys. 26, 306 (1961).

22) Y. Fujiwara, private communication (1989).

23) F. P. Brady, N. S. P. King, B. E. Bonner, M. W. McNaughton, J. C. Wang and W. W. True, Phys. Rev. C16, 31 (1977).

Table 1 Measured c.m. differential cross sections for the reactions $^{6}Li(n,d)^{5}He$ and $^{6}Li(n,t)^{4}He$ at 14.1 MeV.

Telescope setting angle θ_0 (deg)	$^{6}Li(n,d)^{5}He$		$^{6}Li(n,t)^{4}He$		Ref.
	C.m. mean angle Θ_d +) (deg)	$d\sigma(\Theta_d)/d\Omega$ ++) (mb/sr)	C.m. mean angle Θ_t (deg)	$d\sigma(\Theta_t)/d\Omega$ (mb/sr)	
0	8 ± 5 a)	48.2 ± 2.4 b)	8 ± 4 a)	7.4 ± 0.5 b)	1)
14	18 ± 8	39.3 ± 2.0	17 ± 8	5.5 ± 0.4	1)
22	27 ± 8	30.0 ± 1.5	28 ± 9	2.7 ± 0.2	1)
30	35 ± 7	24.6 ± 1.3	36 ± 7	2.1 ± 0.2	1)
40	50 ± 6	10.2 ± 0.5	50 ± 7	2.0 ± 0.2	1)
50	62 ± 6	7.3 ± 0.4	64 ± 6	1.5 ± 0.2	1)
60	74 ± 5	3.0 ± 0.3	71 ± 5	1.3 ± 0.2	1)
93	110 ± 5	1.4 ± 0.5	110 ± 5	1.8 ± 0.2	2)
100	116 ± 4	2.5 ± 0.6	117 ± 4	1.7 ± 0.2	2)
115	130 ± 4	5.0 ± 0.8	131 ± 4	1.4 ± 0.1	3)
130	144 ± 3	6.4 ± 2.0	145 ± 3	1.7 ± 0.3	2,3)
17			157 ± 9	1.3 ± 0.10 c)	1)
11			165 ± 9	2.0 ± 0.14 c)	1)
3			172 ± 6	2.3 ± 0.14 c)	1,2)

+) The angle corresponding to ^{5}He(g.s.).

++) The cross section has been corrected for an unobserved low-energy part by means of the n-α FSI theory.

a) HWHM of the calculated angular frequency distribution.

b) The error includes the systematic overall error (±4.8%) in addition to the statistical error.

c) The data from the alpha particle measurement.

Table 2 Optical potential parameters used in the EFR-DWBA calculations. The potential form expression is the same as that given in ref. 1.

	Entrance channels		Exit channels			
	n-^{6}Li	n-^{7}Li	d-^{5}He	d-^{6}He	t-^{4}He	t-^{5}He
Potential depth parameters:						
V (MeV)	37.3	37.0	115.0	92.5	138.0	138.0
W (MeV)	19.2^{G}	19.0^{G}	0.68^{S}	72.4^{S}	2.0^{V}	2.0^{V}
V_{so} (MeV)	31.2	18.8	0.0	17.2	9.2	18.8
Range parameters:						
r_0 (fm)	1.63	1.60	1.26	2.17	0.93	1.10
r_0' (fm)	1.43	1.43	1.80	2.35	2.00	2.00
a (fm)	0.53	0.50	0.73	0.61	0.70	0.70
b (fm)	0.55	0.40	0.31	0.61	0.65	0.65
r_c (fm)	0.00	0.00	1.40	1.40	1.40	1.40
Ref.	14	14	1	5	1	5

G: Gauss form. S: Surface Woods-Saxon form. V: Volume Woods-Saxon form.

Table 3 Measured c.m. differential cross sections for the reactions $^{7}Li(n,d)^{6}He(g.s.)$ and $^{7}Li(n,d)^{6}He^{*}(1st)$ at 14.1 MeV.

Telescope setting angle θ_0 (deg)	$^{7}Li(n,d_0)^{6}He(g.s.)$		$^{7}Li(n,d_1)^{6}He^{*}(1st)$		Ref.
	C.m. mean angle θ_d +) (deg)	$d\sigma(\theta_d)/d\Omega$ (mb/sr)	C.m. mean angle θ_d ++) (deg)	$d\sigma(\theta_d)/d\Omega$ (mb/sr)	
0	8 ± 5 a)	0.7 ± 0.4 b)	8 ± 5 a)	0.8 ± 0.5 b)	6)
	8 ± 5	2.0 ± 0.8	9 ± 4	2.5 ± 0.9	5)
5	10 ± 8	2.0 ± 0.8	11 ± 8	2.7 ± 1.0	5)
10	13 ± 9	1.5 ± 0.6	13 ± 9	1.0 ± 0.6	6)
	15 ± 8	2.6 ± 1.1	16 ± 9	2.8 ± 1.0	5)
20	25 ± 9	2.4 ± 0.6	27 ± 9	0.6 ± 0.4	6)
	27 ± 7	1.4 ± 0.4	29 ± 7	2.5 ± 0.9	5)
30	41 ± 8	1.0 ± 0.6	44 ± 8	0.4 ± 0.6	6)
	40 ± 6	1.4 ± 0.6	43 ± 7	1.9 ± 0.9	5)
40	52 ± 8	0.4 ± 0.3	56 ± 8	0.2 ± 0.3	6)
	53 ± 6	0.9 ± 0.5	57 ± 6	0.0 ± 0.7	5)
50	65 ± 7	0.2 ± 0.4	71 ± 7	0.1 ± 0.4	6)
	66 ± 5	1.1 ± 0.7	71 ± 5		5)
60	78 ± 6	0.6 ± 0.4	83 ± 6		6)
80	100 ± 4	0.2 ± 0.3	107 ± 4		6)

+) The c.m. angle calculated for the reaction $^{7}Li(n,d_0)^{6}He(g.s.)$ of Q = -7.753 MeV.

++) The c.m. angle calculated for the reaction $^{7}Li(n,d_1)^{6}He^{*}(1st)$ of Q = -9.553 MeV.

a) HWHM of the calculated angular frequency distribution.

b) The error is the statistical error only.

Table 4 Measured c.m. differential cross section for the reaction $^{7}Li(n,t)^{5}He$ at 14.1 MeV.

Telescope setting angle θ_0 (deg)	Lab. mean angle θ_t (deg)	C.m. mean angle Θ_t +) (deg)	$d\sigma(\Theta_t)/d\Omega$ *) ($E_t \geq 3.2$ MeV) (mb/sr)	$d\sigma(\Theta_t)/d\Omega$ **) (mb/sr)	Ref.
0	5.8	7.8 ± 5. a)	20.7 ± 0.6 b)	11.7 ± 1.1 c)	6)
0	6.3	8.1 ± 5.	23.4 ± 0.9		5)
0	7.3	9.4 ± 5.		14.5 ± 1.2	4)
5	7.6	10.1 ± 5.	19.4 ± 0.9		5)
5	8.5	11.4 ± 5.		13.8 ± 1.1	4)
10	9.4	12.6 ± 5.	20.9 ± 0.6	12.9 ± 1.2	6)
10	11.1	14.8 ± 7.	19.3 ± 0.9		5)
15	15.9	21.4 ± 7.		5.0 ± 0.5	4)
20	18.2	24.4 ± 7.	16.2 ± 0.6	10.4 ± 1.0	6)
20	20.3	26.8 ± 7.	16.9 ± 0.9		5)
25	25.3	33.7 ± 7.		4.8 ± 0.5	4)
30	30.4	40.4 ± 7.	14.4 ± 0.6	5.0 ± 0.7	6)
30	30.1	40.0 ± 6.	15.8 ± 0.9		5)
35	35.0	46.4 ± 7.		5.5 ± 0.5	4)
40	39.2	51.8 ± 7.	10.6 ± 0.5	6.6 ± 0.9	6)
40	39.9	52.7 ± 6.	15.1 ± 0.8		5)
45	44.8	58.9 ± 6.		7.0 ± 0.6	4)
50	49.2	64.3 ± 6.	14.7 ± 0.3	6.7 ± 0.9	6)
50	49.8	65.1 ± 5.	12.0 ± 0.8		5)
55	54.7	71.1 ± 6.		5.4 ± 0.6	4)
60	60.1	77.5 ± 6.	7.5 ± 0.5	2.9 ± 0.6	6)
60	59.8	77.2 ± 5.	7.1 ± 0.7		5)
65	64.7	82.9 ± 5.		3.1 ± 0.5	4)
70	69.8	88.7 ± 5.	3.6 ± 0.7		5)
80	79.5	99.3 ± 5.	5.3 ± 0.5	2.4 ± 0.7	6)
80	79.8	99.6 ± 5.	2.6 ± 0.7		5)
90	89.9	110.1 ± 5.	2.2 ± 0.7		5)

*) The cross section for tritons of energies larger than 3.2 MeV.

**) The cross section for the reaction channel $^{7}Li(n,t)n\alpha$ with the n-α FSI only.

+) The c.m. angle calculated for the $^{7}Li(n,t)\ ^{5}He(g.s.)$ of Q = -3.360 MeV.

a) HWHM of the calculated angular frequency distribution.

b) The error does not include the systematic error of the correction for an unobserved part of the spectrum by means of the n-α FSI theory.

Table 5 Spectroscopic factors $S^{z}_{xy}(a)$ extracted in this work assuming $S^{d}_{np}(1s) = 1.00$ and $S^{t}_{nd} = 1.50$.
$S^{z}_{xy}(a_j) = \langle T'T_z'\tau\tau_z|TT_z\rangle^2 S(lj)$ for a system z (isotopic spin T, the z component T_z) made up of clusters x (τ,τ_z) and y (T', T_z') in relative motion state a_j with the transferred orbital angular momentum l and total angular momentum j, where S(lj) is the spectroscopic factor of Cohen and Kurath[17].

	This work				Theory				Ref.
a_j =	$2s_1$	$1d_3$	$1p_{3/2}$	$1p_{1/2}$	$2s_1$	$1d_3$	$1p_{3/2}$	$1p_{1/2}$	
z = ^{6}Li(1^+):									
$S^{6Li}_{p5He(3/2^-)}$			0.91	0.93			0.82	0.82	18)
							0.32	0.34	17)
$S^{6Li}_{d4He(0^+)}$	0.75	0.07			1.00[a]				20)
					0.75	0.75			21)
					1.13				22)
z = ^{7}Li($3/2^-$):									
$S^{7Li}_{p6He(0^+)}$			1.0				0.59		17)
			- 0.8				0.50		19)
$S^{7Li}_{p6He(2^+)}$			1.0				0.22	0.18	17)
			- 0.6				0.10		19)
$S^{7Li}_{d5He(3/2^-)}$	0.8	0.4			0.45[a]	0.45[a]			20)
	- 1.0				0.80[b]	0.80[b]			21)
					1.26	1.27			22)

a The two-particle coefficients of fractional parentage (c.f.p.).

b ^{7}Li = t + ^{4}He.

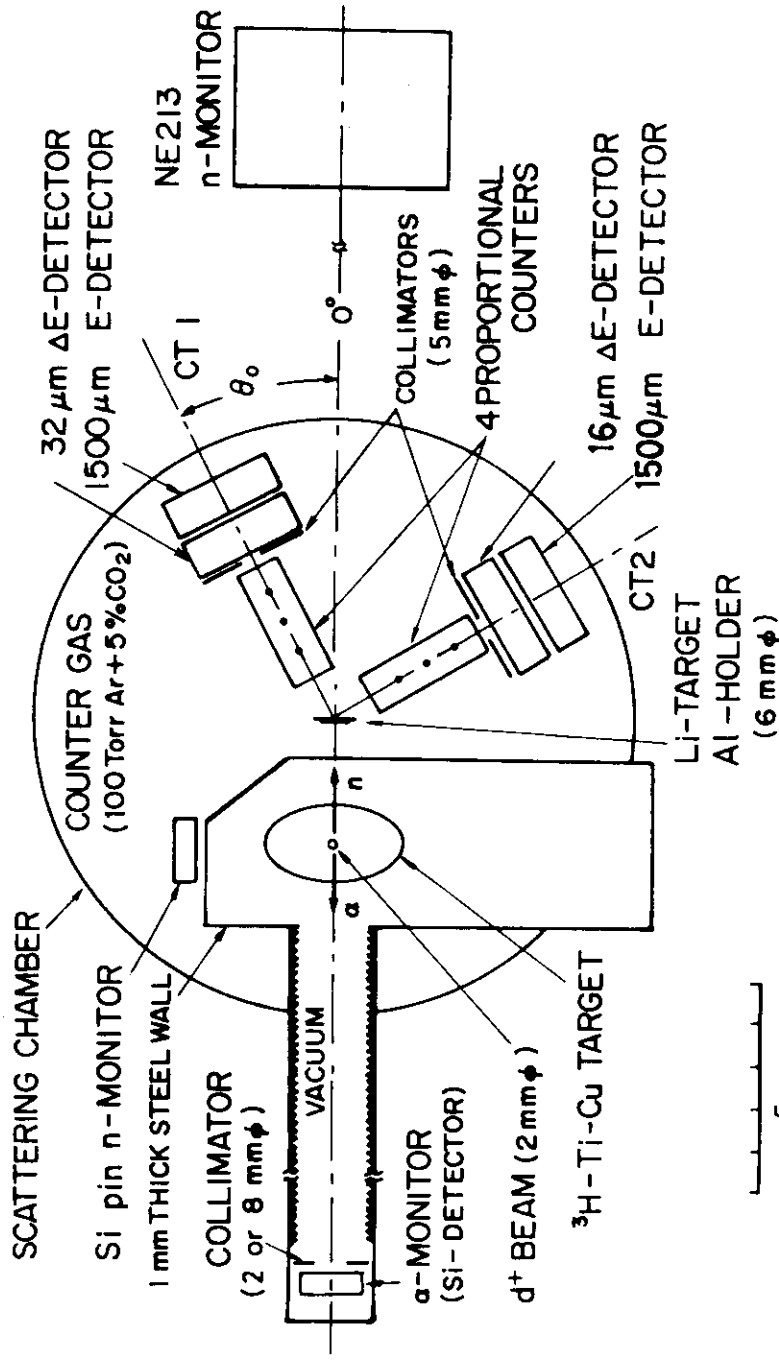

Fig. 1 Experimental layout.

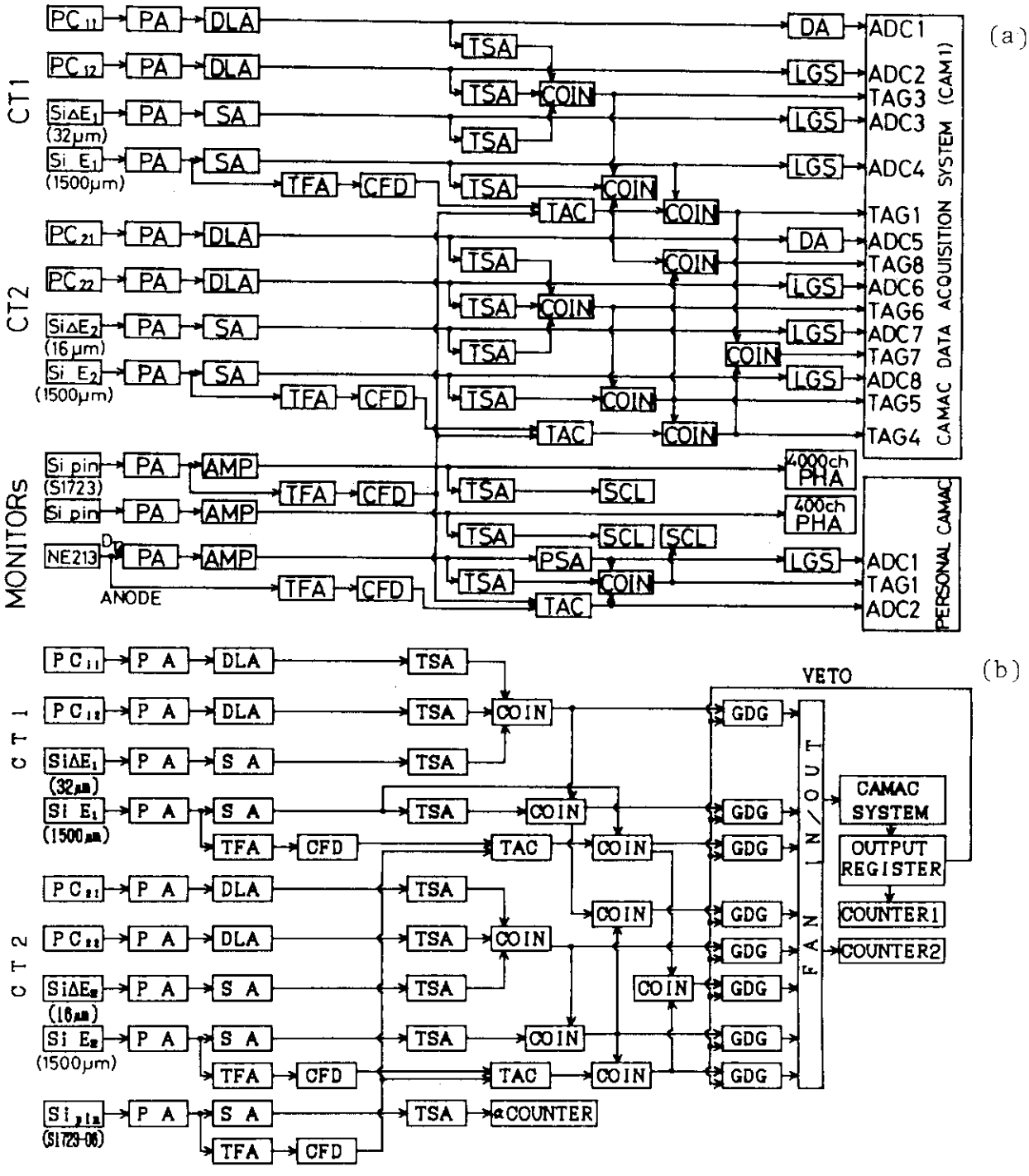

Fig. 2 Block diagrams of (a) the main electronic system including the α-monitor for T-d neutrons and (b) the timing and counting loss monitoring system. PA, SA, DLA, AMP and DA: amplifiers; TFA: timing filter amplifier; TSA: timing single channel analyzer; CFD: discriminator; COIN: coincidence circuit; TAC: time-to-amplitude converter; LGS: linear gate stretcher; PHA: pulse-height analyzer; SCL: scaler.

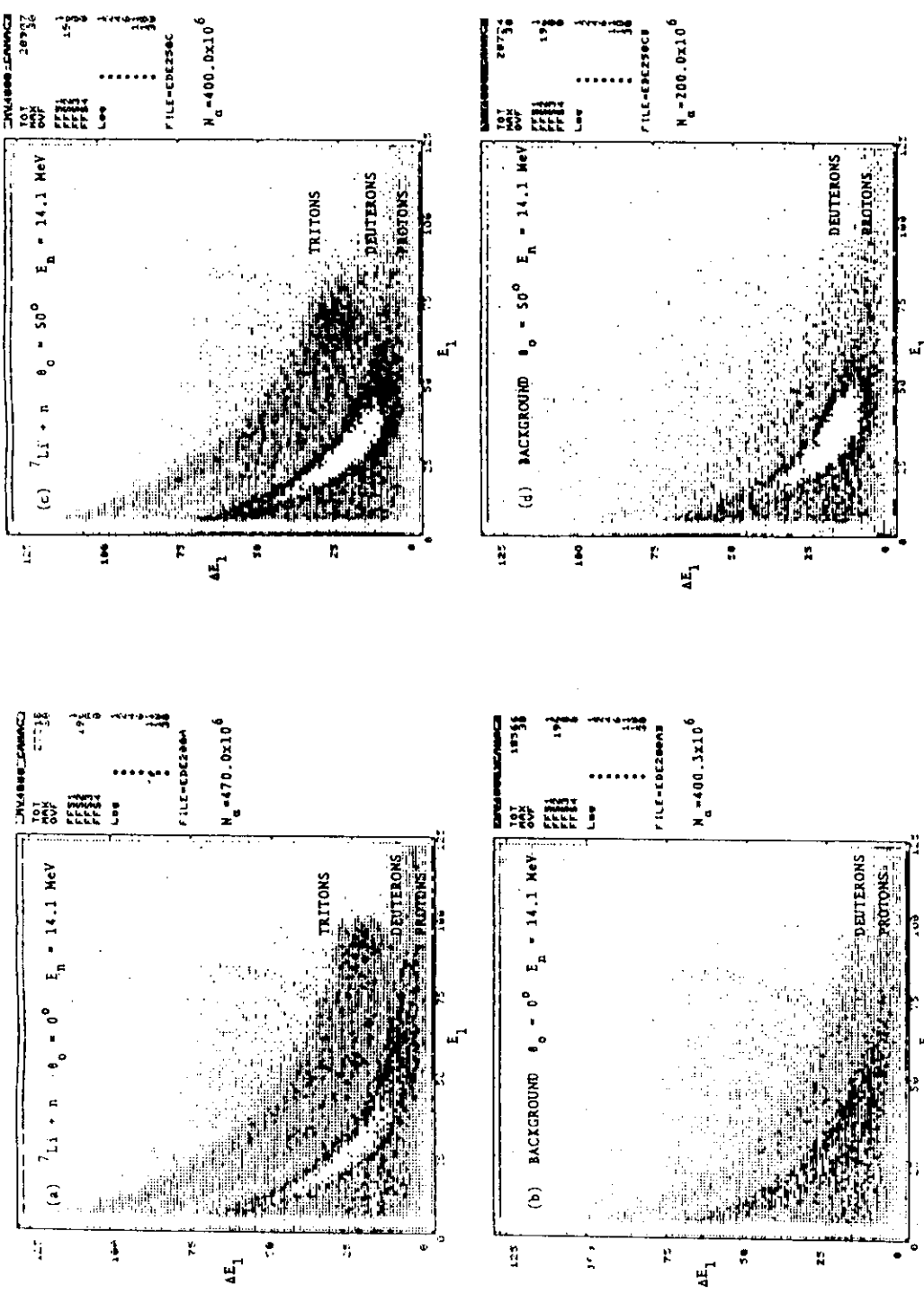

Fig. 3 Typical examples of the ΔE vs E display for particle identification.
(a) The particle distribution measured by CT1 at 0° with ^{7}Li.
(b) The background distribution measured by CT1 at 0° without ^{7}Li.
(c) The particle distribution measured by CT2 at 50° with ^{7}Li.
(d) The background distribution measured by CT2 at 50° without ^{7}Li.

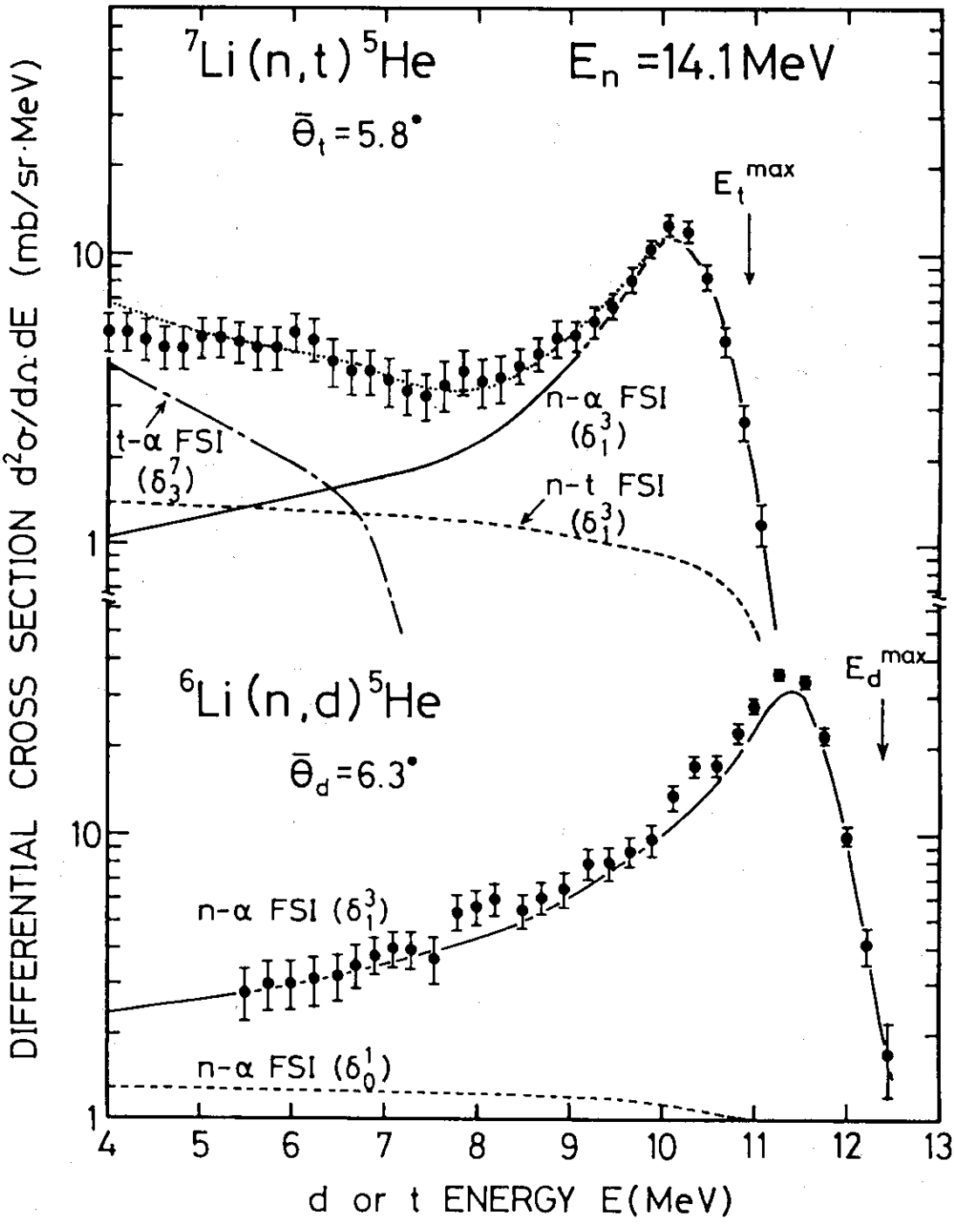

Fig. 4 Typical examples of measured and calculated deuteron- and triton-energy spectra from the ^{6}Li(n,d)^{5}He reaction at 6.3° and the ^{7}Li(n,t)^{5}He reaction at 5.8°, respectively. δ_L^{2J} represents the phase shift of L-wave scattering in a final subsystem of total angular momentum J.

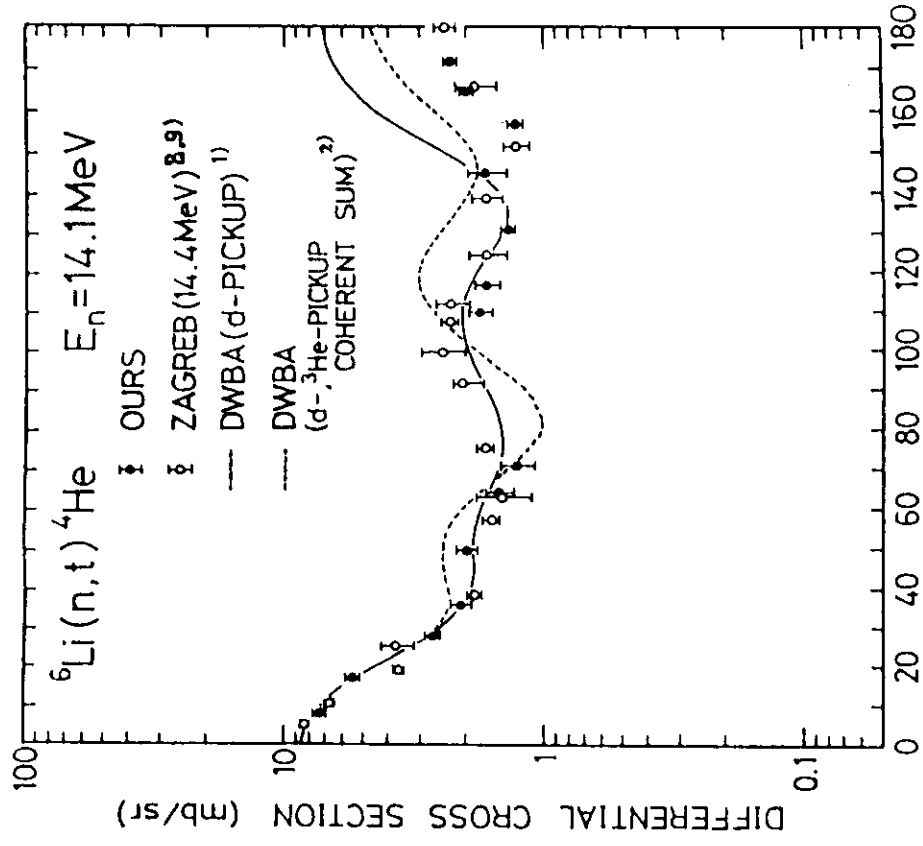

Fig. 6 Measured and calculated C.M. angular distributions of tritons from the ^{6}Li(n,t)^{4}He reaction at 14.1 MeV.

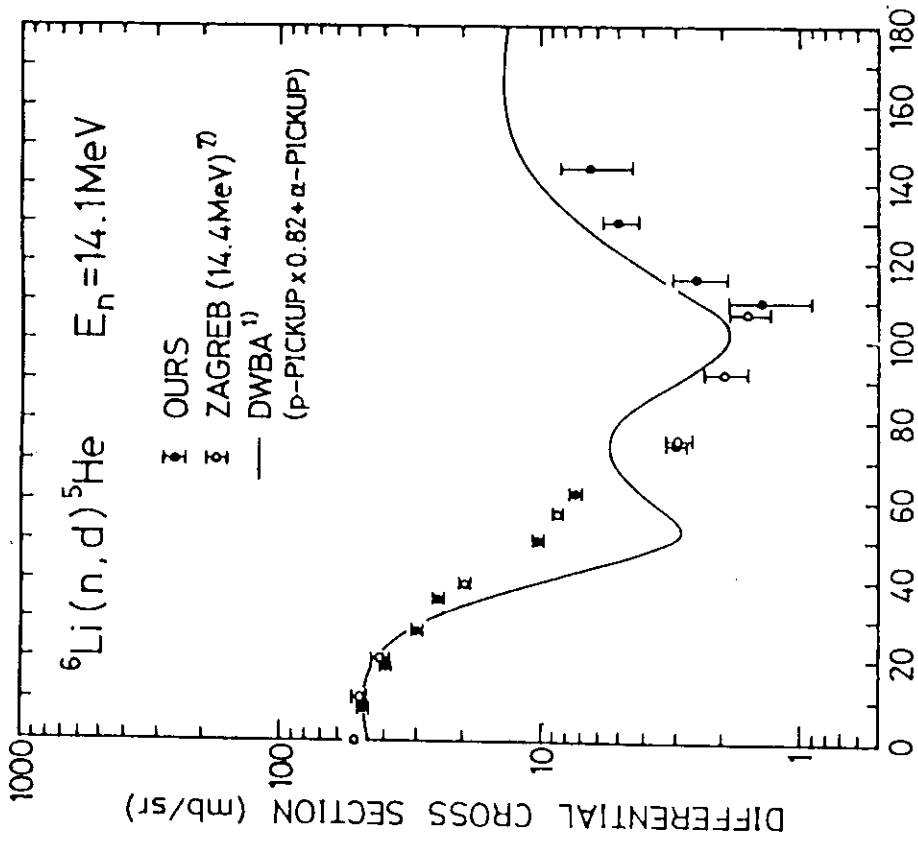

Fig. 5 Measured and calculated C.M. angular distributions of deuterons from the ^{6}Li(n,d)^{5}He reaction at 14.1 MeV.

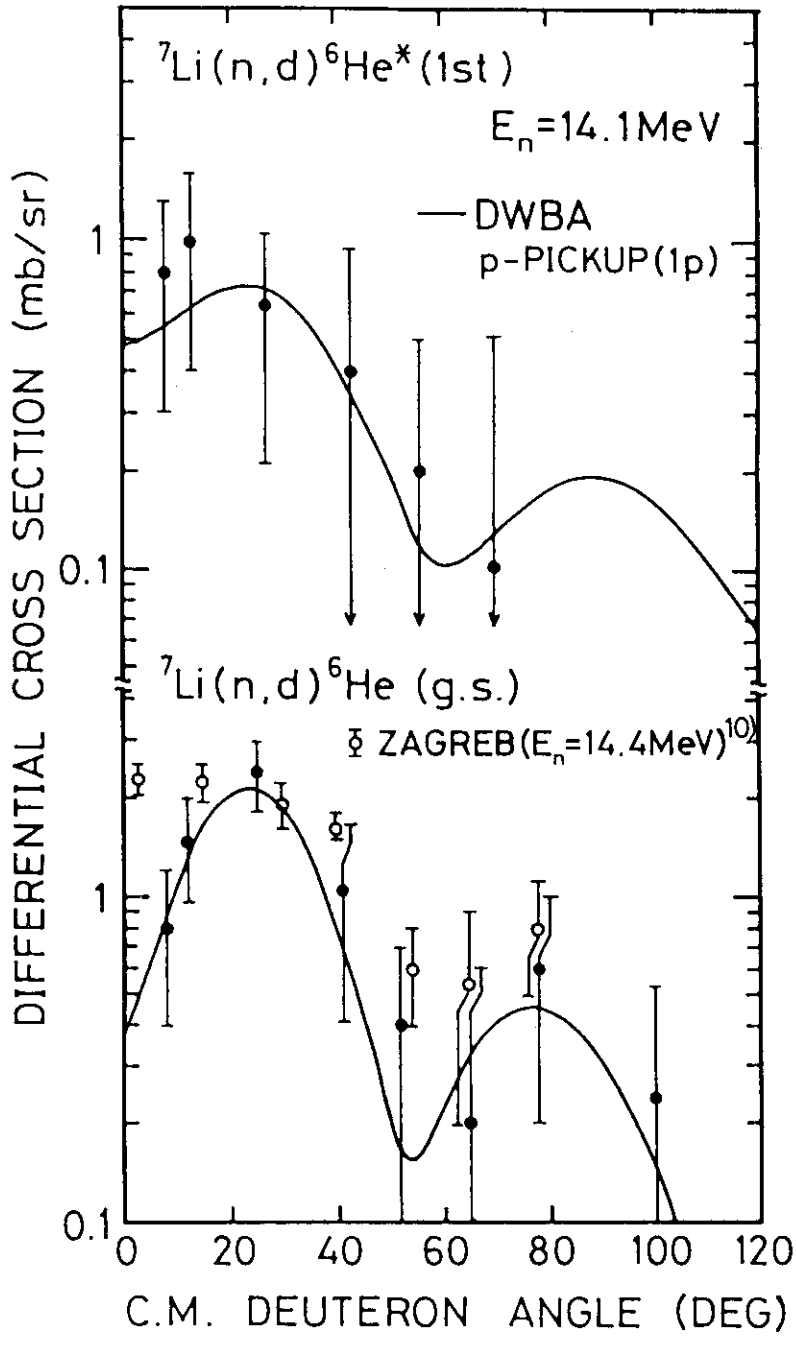

Fig. 7 Measured and calculated C.M. angular distributions of deuterons from the reactions ^{7}Li(n,d_0)^{6}He(g.s.) and ^{7}Li(n,d_1)^{6}He*(1st) at 14.1 MeV.

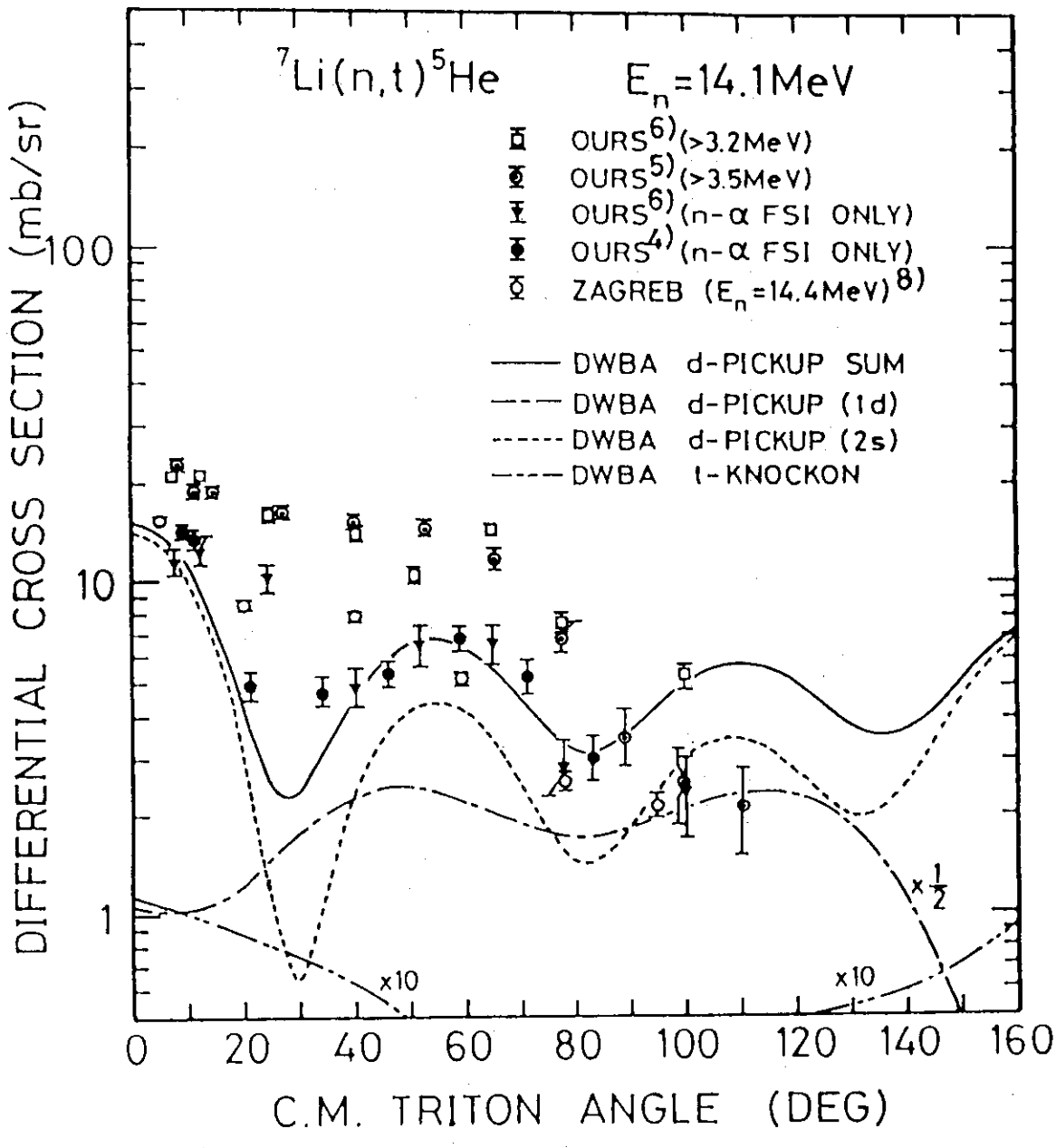

Fig. 8 Measured and calculated C.M. angular distributions of tritons from the $^{7}Li(n,t)^{5}He$ reaction at 14.1 MeV.

Appendix

Table A1 Measured deuteron energy spectra from the reaction $^{6}Li(n,d)^{5}He$ at 14.1 MeV. (The data from fig. 3 in ref. 1.)

$\bar{\theta}_d$ = 6.3°		$\bar{\theta}_d$ = 13.7°		$\bar{\theta}_d$ = 20.7°		$\bar{\theta}_d$ = 27.1°	
E_d (MeV)	$d^2\sigma/d\Omega \cdot dE_d$ (mb/sr·MeV)	E_d (MeV)	$d^2\sigma/d\Omega \cdot dE_d$ (mb/sr·MeV)	E_d (MeV)	$d^2\sigma/d\Omega \cdot dE_d$ (mb/sr·MeV)	E_d (MeV)	$d^2\sigma/d\Omega \cdot dE_d$ (mb/sr·MeV)
6.94	3.82 ± 0.64	7.27	5.02 ± 0.75	7.27	3.38 ± 0.61	7.28	3.86 ± 0.47
7.05	3.95 ± 0.66	7.39	4.47 ± 0.77	7.38	3.44 ± 0.62	7.39	3.98 ± 0.48
7.17	4.23 ± 0.68	7.50	5.07 ± 0.75	7.49	3.34 ± 0.62	7.51	3.99 ± 0.48
7.28	3.38 ± 0.60	7.61	4.92 ± 0.75	7.61	3.55 ± 0.63	7.62	4.00 ± 0.49
7.39	4.50 ± 0.71	7.73	4.78 ± 0.74	7.72	3.48 ± 0.63	7.73	4.19 ± 0.50
7.51	3.09 ± 0.57	7.84	4.84 ± 0.75	7.84	3.42 ± 0.63	7.85	3.62 ± 0.49
7.62	4.21 ± 0.68	7.96	4.75 ± 0.74	7.95	4.64 ± 0.73	7.96	3.65 ± 0.49
7.74	4.90 ± 0.75	8.07	4.67 ± 0.74	8.07	2.71 ± 0.60	8.08	3.66 ± 0.50
7.85	5.88 ± 0.83	8.19	5.93 ± 0.83	8.18	4.43 ± 0.77	8.19	3.52 ± 0.50
7.97	5.31 ± 0.78	8.30	5.56 ± 0.86	8.30	5.55 ± 0.87	8.31	3.69 ± 0.50
8.08	6.00 ± 0.84	8.42	4.30 ± 0.76	8.41	3.50 ± 0.70	8.42	4.57 ± 0.56
8.20	6.83 ± 0.90	8.53	3.44 ± 0.69	8.53	2.88 ± 0.63	8.54	4.77 ± 0.58
8.31	5.43 ± 0.79	8.65	3.37 ± 0.69	8.64	4.80 ± 0.82	8.65	4.32 ± 0.55
8.43	4.73 ± 0.79	8.76	5.50 ± 0.87	8.76	5.84 ± 0.90	8.77	5.25 ± 0.63
8.54	6.43 ± 0.93	8.88	5.07 ± 0.84	8.88	3.78 ± 0.72	8.88	4.95 ± 0.61
8.66	5.14 ± 0.84	9.00	4.81 ± 0.82	8.99	5.10 ± 0.86	9.00	5.60 ± 0.64
8.78	5.17 ± 0.85	9.11	6.39 ± 0.94	9.11	6.35 ± 0.97	9.12	5.77 ± 0.67
8.89	6.66 ± 0.96	9.23	6.10 ± 0.95	9.22	5.13 ± 0.86	9.23	6.17 ± 0.71
9.01	5.96 ± 0.91	9.34	6.23 ± 0.96	9.34	3.99 ± 0.78	9.35	5.27 ± 0.65
9.12	6.62 ± 0.96	9.46	5.51 ± 0.90	9.46	6.43 ± 1.00	9.46	6.11 ± 0.70
9.24	9.76 ± 1.17	9.58	6.66 ± 1.01	9.57	6.56 ± 1.01	9.58	7.23 ± 0.78
9.36	7.34 ± 1.04	9.69	7.04 ± 1.05	9.69	7.74 ± 1.10	9.70	7.46 ± 0.77
9.47	8.72 ± 1.14	9.81	6.92 ± 1.04	9.81	8.96 ± 1.20	9.81	6.96 ± 0.75
9.59	9.88 ± 1.21	9.93	8.35 ± 1.15	9.92	8.20 ± 1.13	9.93	7.47 ± 0.78
9.71	7.74 ± 1.10	10.04	7.44 ± 1.09	10.04	8.00 ± 1.12	10.05	7.93 ± 0.78
9.82	8.70 ± 1.18	10.16	6.76 ± 1.02	10.16	10.55 ± 1.29	10.16	11.29 ± 0.91
9.94	10.97 ± 1.33	10.28	9.69 ± 1.24	10.27	13.93 ± 1.46	10.28	11.17 ± 0.89
10.06	13.10 ± 1.46	10.39	11.28 ± 1.34	10.39	14.86 ± 1.47	10.40	11.96 ± 0.91
10.17	14.27 ± 1.55	10.51	15.68 ± 1.55	10.51	15.90 ± 1.50	10.51	11.17 ± 0.87
10.29	17.01 ± 1.66	10.63	15.51 ± 1.50	10.62	18.32 ± 1.60	10.63	12.56 ± 0.91
10.41	18.04 ± 1.73	10.74	19.42 ± 1.66	10.74	19.20 ± 1.62	10.75	13.04 ± 0.93
10.52	16.31 ± 1.63	10.86	18.00 ± 1.51	10.86	22.83 ± 1.74	10.86	11.45 ± 0.87
10.64	19.12 ± 1.73	10.98	22.95 ± 1.77	10.97	20.12 ± 1.63	10.98	9.40 ± 0.79
10.76	20.20 ± 1.72	11.09	26.28 ± 1.86	11.09	16.97 ± 1.50	11.10	7.69 ± 0.71
10.87	24.96 ± 1.89	11.21	28.18 ± 1.93	11.21	15.88 ± 1.45	11.21	5.60 ± 0.61
10.99	26.97 ± 1.94	11.33	25.84 ± 1.85	11.33	12.87 ± 1.30	11.33	3.09 ± 0.46
11.11	29.29 ± 2.01	11.45	23.79 ± 1.77	11.44	7.39 ± 1.00	11.45	2.17 ± 0.39
11.23	34.83 ± 2.15	11.56	22.66 ± 1.73	11.56	5.49 ± 0.86	11.57	1.64 ± 0.34
11.34	37.01 ± 2.21	11.68	14.40 ± 1.39	11.68	2.36 ± 0.57	11.68	0.74 ± 0.23
11.46	33.56 ± 2.11	11.80	8.59 ± 1.07	11.80	2.09 ± 0.54	11.80	0.06 ± 0.07
11.58	33.41 ± 2.11	11.92	6.43 ± 0.94	11.91	0.62 ± 0.30	11.92	0.00 ± 0.00
11.70	28.75 ± 1.96	12.03	6.14 ± 0.92	12.03	0.96 ± 0.38	12.04	0.00 ± 0.00
11.81	15.88 ± 1.46	12.15	3.09 ± 0.67	12.15	0.23 ± 0.19		
11.93	13.41 ± 1.34	12.27	2.03 ± 0.56	12.27	0.11 ± 0.13		
12.05	6.43 ± 0.94	12.39	1.39 ± 0.47	12.38	0.05 ± 0.13		
12.17	5.74 ± 0.89	12.50	0.64 ± 0.33	12.50	0.00 ± 0.00		
12.28	2.60 ± 0.62	12.62	0.28 ± 0.35				
12.40	1.91 ± 0.54	12.74	1.09 ± 0.38				
12.52	1.50 ± 0.49	12.86	0.09 ± 0.00				
12.64	0.96 ± 0.41	12.98	0.27 ± 0.53				
12.76	0.14 ± 0.24	13.09	0.00 ± 0.00				
12.87	0.00 ± 0.00						

The error is given in FWHM.

The corrections have been carried out for background, energy losses of deuterons in the target and the counter gas, and degraded neutron effects.

Table A2 Measured triton energy spectra from the reaction $^{7}Li(n,t)^{5}He$ at 14.1 MeV. (The data from ref. 6.)

θ_t = 5.8°		9.4°	18.2°	30.4°	39.2°
E_t (MeV)	$d^2\sigma/d\Omega dE_t$ (mb/srMeV)	$d^2\sigma/d\Omega dE_t$ (mb/srMeV)	$d^2\sigma/d\Omega dE_t$ (mb/srMeV)	$d^2\sigma/d\Omega dE_t$ (mb/srMeV)	$d^2\sigma/d\Omega dE_t$ (mb/srMeV)
3.2	6.4±0.9	6.1±0.9	6.5±0.9	5.7±0.9	3.3±0.6
3.4	5.4±0.8	4.8±0.8	5.2±0.8	6.1±0.9	3.5±0.7
3.6	5.2±0.8	4.4±0.8	3.7±0.7	6.7±0.9	2.3±0.6
3.8	5.3±0.8	4.8±0.7	2.3±0.6	6.0±0.8	2.0±0.6
4.0	5.4±0.8	5.7±0.8	2.1±0.6	5.5±0.8	1.6±0.4
4.2	5.4±0.8	5.8±0.8	2.8±0.7	4.7±0.7	1.0±0.4
4.4	5.1±0.8	5.5±0.8	3.0±0.7	3.4±0.7	1.1±0.5
4.6	4.8±0.8	5.1±0.8	2.2±0.7	2.8±0.7	0.7±0.3
4.8	4.8±0.8	4.5±0.7	1.5±0.7	2.5±0.7	0.7±0.3
5.0	5.2±0.8	5.0±0.7	1.8±0.7	2.0±0.7	1.7±0.6
5.2	5.2±0.8	5.0±0.8	1.8±0.7	1.5±0.7	1.5±0.5
5.4	5.0±0.8	5.4±0.8	2.0±0.7	2.8±0.8	1.3±0.4
5.6	4.8±0.8	4.7±0.8	2.1±0.8	3.1±0.8	1.2±0.4
5.8	4.8±0.8	5.6±0.8	3.6±0.8	2.8±0.7	1.3±0.4
6.0	5.4±0.8	6.6±0.8	4.4±0.8	4.2±0.8	1.8±0.5
6.2	5.1±0.7	6.2±0.8	2.6±0.7	4.0±0.8	1.1±0.4
6.4	4.3±0.7	4.5±0.7	2.4±0.7	3.3±0.8	1.4±0.4
6.6	4.0±0.7	3.4±0.7	2.3±0.7	3.6±0.7	1.5±0.4
6.8	4.0±0.7	3.0±0.6	2.8±0.7	3.6±0.7	1.1±0.3
7.0	3.7±0.7	2.7±0.6	3.6±0.7	3.2±0.7	1.7±0.5
7.2	3.4±0.6	2.7±0.6	3.6±0.7	2.5±0.7	1.7±0.6

Table A2 (continued).

θ_t = 5.8°	9.4°	18.2°	30.4°	39.2°
E_t (MeV)	$d^2\sigma/d\Omega dE_t$ (mb/srMeV)	$d^2\sigma/d\Omega dE_t$ (mb/srMeV)	$d^2\sigma/d\Omega dE_t$ (mb/srMeV)	$d^2\sigma/d\Omega dE_t$ (mb/srMeV)	$d^2\sigma/d\Omega dE_t$ (mb/srMeV)
7.4	3.3±0.6	2.6±0.6	4.0±0.7	1.6±0.6	1.5±0.6
7.6	3.6±0.7	2.7±0.6	3.2±0.7	1.9±0.6	1.0±0.4
7.8	4.0±0.7	2.6±0.6	4.2±0.7	3.3±0.7	2.6±0.4
8.0	3.7±0.7	4.4±0.7	5.9±0.7	3.7±0.6	4.2±0.6
8.2	3.8±0.7	4.1±0.7	5.5±0.7	3.5±0.6	4.8±0.6
8.4	4.2±0.6	4.0±0.6	5.3±0.7	5.0±0.6	6.2±0.7
8.6	4.6±0.6	3.8±0.6	6.1±0.7	5.9±0.7	6.4±0.7
8.8	5.1±0.7	4.5±0.6	6.6±0.7	5.5±0.6	6.2±0.7
9.0	5.2±0.6	4.8±0.6	6.1±0.7	5.6±0.6	6.0±0.7
9.2	5.9±0.7	5.6±0.6	7.9±0.7	5.8±0.6	4.6±0.6
9.4	6.7±0.7	7.3±0.7	9.4±0.8	4.9±0.6	2.7±0.4
9.6	8.2±0.8	9.7±0.8	10.1±0.8	3.2±0.5	1.6±0.3
9.8	10.6±0.9	13.1±0.9	9.7±0.8	2.0±0.4	1.0±0.3
10.0	12.4±0.9	13.4±1.0	7.6±0.7	1.0±0.3	0.5±0.2
10.2	11.8±0.9	11.5±0.9	5.7±0.6	0.5±0.1	0.3±0.1
10.4	8.4±0.8	8.5±0.8	3.0±0.4	0.2±0.0	0.1±0.0
10.6	5.1±0.6	4.8±0.5	1.8±0.3	0.1±0.0	
10.8	2.7±0.4	1.8±0.3	1.1±0.2		
11.0	1.2±0.2	0.6±0.1	0.4±0.1		
Σ	44.2±1.0	44.1±1.0	34.7±0.9	27.9±0.9	17.2±0.7 (mb/sr)

The error is given in FWHM.

The corrections have been carried out for background, energy losses of tritons in the target and the counter gas, and degraded neutron effects.

Table A2 (continued).

θ_t = 49.2°		60.2°	79.5°
E_t (MeV)	$d^2\sigma/d\Omega dE_t$ (mb/srMeV)	$d^2\sigma/d\Omega dE_t$ (mb/srMeV)	$d^2\sigma/d\Omega dE_t$ (mb/srMeV)
3.2	5.4±0.4	3.7±0.8	1.4±0.6
3.4	3.6±0.4	2.6±0.7	1.3±0.6
3.6	2.9±0.4	2.1±0.7	1.5±0.5
3.8	2.8±0.4	2.0±0.6	1.5±0.5
4.0	3.1±0.3	2.3±0.6	1.5±0.5
4.2	2.9±0.4	2.1±0.6	1.4±0.5
4.4	2.9±0.4	1.5±0.6	1.2±0.5
4.6	3.4±0.4	1.4±0.6	0.9±0.3
4.8	3.5±0.4	1.7±0.6	0.4±0.3
5.0	3.2±0.4	1.7±0.6	0.9±0.5
5.2	2.9±0.4	1.3±0.6	1.4±0.6
5.4	3.0±0.4	1.2±0.6	1.5±0.7
5.6	3.1±0.4	1.5±0.6	1.8±0.6
5.8	3.3±0.3	1.9±0.5	1.7±0.5
6.0	3.2±0.3	2.1±0.5	1.3±0.6
6.2	2.9±0.3	2.1±0.6	1.2±0.5
6.4	2.8±0.4	2.1±0.6	0.9±0.3
6.6	2.6±0.3	2.2±0.6	0.6±0.2
6.8	2.9±0.3	2.5±0.6	
7.0	3.5±0.3	2.1±0.6	
7.2	4.2±0.4	1.6±0.5	
7.4	5.0±0.3	1.5±0.5	

Table A2 (continued).

θ_t = 49.2°		60.2°	79.5°
E_t (MeV)	$d^2\sigma/d\Omega dE_t$ (mb/srMeV)	$d^2\sigma/d\Omega dE_t$ (mb/srMeV)	$d^2\sigma/d\Omega dE_t$ (mb/srMeV)
7.6	5.2±0.3	1.2±0.3	
7.8	5.9±0.3	0.6±0.3	
8.0	6.1±0.4	0.2±0.1	
8.2	5.4±0.4	0.1±0.0	
8.4	4.4±0.3		
8.6	3.2±0.3		
8.8	2.1±0.3		
9.0	1.6±0.2		
9.2	1.1±0.2		
9.4	0.4±0.2		
9.6	0.2±0.1		
9.8	0.1±0.1		
10.0	0.1±0.1		
Σ	23.1±0.4	10.1±0.6	5.7±0.5 (mb/sr)

The error is given in FWHM.

The corrections have been carried out for background, energy losses of tritons in the target and the counter gas, and degraded neutron effects.